DOUBLE-DIFFUSIVE CONVECTION MHD FLOW OF A SECOND GRADE FLUID WITH NEWTONIAN HEATING IN THE PRESENCE OF ELASTIC DEFORMATION IN A POROUS MEDIUM WITH SORET AND CHEMICAL REACTION

Supported by tetfund TERTIARY EDUCATION TRUST FUND

J.A. Gbadeyan*, A.S. Idowu and M.A. Olanrewaju
Department of Mathematics, University of Ilorin, Ilorin, Kwara State, Nigeria
*Corresponding author: anuoluwapoolanrewaju2012@yahoo.com

Abstract: The double-diffusive convection MHD flow of a second grade fluid with a convective surface boundary condition in the presence of elastic deformation in a porous medium with Soret and chemical reaction over a stretching sheet are investigated. The particular attraction lies in searching the effects of a second grade fluid parameter, elastic deformation, chemical reaction parameter and the diffusion thermo on the flow. The governing nonlinear partial differential equations for the flow, heat and mass transfer are transformed into a set of coupled nonlinear ordinary differential equations by using similarity variable, which are solved numerically by appl ying Runge–Kutta fourth–fifth order integration scheme in association with quasilinear shooting technique. The novel results for the dimensionless velocity, temperature, concentration are displayed graphically for various parameters that characterize the flow. The local skin friction, Nusselt number and Sherwood number are shown graphically.

Keywords: Double-diffusive MHD flow, second grade fluid, Newtonian heating.

Introduction

In many natural and technological processes, temperature and mass or concentration diffusion act together to create a buoyancy force which drives the fluid and this is known as double-diffusive convection, or combined heat and mass concentration transfer convection. In oceanography, convection processes involve thermal and salinity gradients and this is referred to as thermohaline convection, whilst surface gradients of the temperature and the solute concentration are referred to as Marangoni convection. The term double-diffusive convection is now widely accepted for all processes which involve simultaneous thermal and concentration (solutal) gradients and provides an explanation for a number of natural phenomena. Because of the coupling between the fluid velocity field and the diffusive (thermal and concentration) fields, double-diffusive convection is more complex than the convective flow which is associated with a single diffusive scalar, and much different behaviour may be expected. Such double-diffusive processes occur in many fields, including chemical engineering (drying, cleaning operations, evaporation, condensation, sublimation, deposition of thin films, energy storage in solar ponds, roll-over in storage tanks containing liquefied natural gas, solution mining of salt caverns for crude oil storage, casting of metal alloys and photosynthesis), solid-state physics (solidification of binary alloy and crystal growth), oceanography (melting and cooling near ice surfaces, sea water intrusion into freshwater lakes and the formation of layered or columnar structures during crystallization of igneous intrusions in the Earth's crust), geophysics (dispersion of dissolvent materials or particulate matter in flows), etc. A clear understanding of the nature of the interaction between thermal and mass or concentration buoyancy forces are necessary in order to control these processes. Many researchers (Raptis *et al*., 2004; Hayat *et al*., 2007; Ishak, 2010; Aziz, 2009, 2010) have shown interest in recent years for obtaining self-similar solutions of boundary layer flows with thermal and/or mass diffusion.

The boundary layer flows and heat transfer over a stretching sheet are quite useful in the engineering applications. Specific examples of such flows occur in the extrusion process, glass fiber and paper production, hot rolling, wire drawing, electronic chips, crystal growing, plastic manufactures, and aerodynamic extrusion of plastic sheets. An extensive literature is available for boundary layer flows induced by a stretching sheet (Singh and Sharma, 2009).

A variety of constitutive equations have been suggested to predict the behavior of non-Newtonian fluids in industry and engineering. Amongst these non-Newtonian fluids, there is one simplest model of differential type fluids which is known as second grade fluid (Asghar *et al.*, 2009). This model can describe the normal stress effects even in steady flows. Convection flow has further practical engineering applications such as cooling of polymer films and metallic plates on conveyers. Recently, Yao *et al.* (2011) discussed the flow and heat transfer in a viscous fluid flow over a stretching/shrinking sheet with convective boundary conditions.

The second grade fluid model is the simplest subclass of viscoelastic fluid for which one can reasonably hope to obtain the analytic solution. Even though considerable progress has been made in our understanding of the flow phenomena, more works are needed to understand the effects of the various parameters involved in the non-Newtonian models and the formulation of an accurate method of analysis for anybody shapes of engineering significance. Also, the boundary layer concept for such fluids is of special importance because of its application to many practical problems, among which we cite the possibility of reducing frictional drag on the hulls of ships and submarines. Furthermore, thermal radiation effects and MHD flow problems have assumed an increasing importance at a fundamental fabrication level. Specifically, such flows occurs in electrical power generation, astrophysical flows, solar power technology, space vehicle re-entry and other industrial areas. Related studies regarding the thermal radiation of a gray fluid have been made in the references.

Hayat and Abbas (2008) examined the heat transfer analysis on the MHD flow of a second grade fluid in a channel with porous medium. Hayat *et al.* (2007) studied the influence of thermal radiation on MHD flow of a second grade fluid. Hayat *et al.* (2007) investigated the MHD flow of a second grade fluid in a porous channel.

Olanrewaju and Abbas (2014) considered the corrigendum to convection heat and mass transfer in a hydromagnetic flow of a second grade fluid in the presence of thermal radiation and thermal diffusion. The researcher pointed out several errors in Olajuwon (2011) work and numerical solutions of the problem were provided with interpretations of the physical parameters to give further insight into the problem.

Hayat *et al.* (2011) *investigated* Flow of a second grade fluid with convective boundary conditions. Abdul *et al.* (2013) studied Slip Effects on the Flow of a Second Grade Fluid in a Varying Width Channel with Application to Stenosed Artery. Singh and Agarwal (2012) examined heat transfer in a second grade fluid over an exponentially stretching sheet through porous Medium with thermal radiation and elastic Deformation under the effect of magnetic field. Baris (2003) discussed the flow of a Second-Grade Visco-Elastic Fluid in a Porous Converging Channel.

It may be remarked that earlier studies did not include the effect of mass diffusion. However, in many real boundary layer flows, the flow, and heat transfer and mass diffusion are always coupled. The above study is motivated by the above referenced work. In particular, Singh and Agarwal (2012) who discussed the heat transfer in a second grade fluid over an exponentially stretching sheet through porous medium with thermal radiation and elastic deformation under the effect of magnetic field. The inclusion of the effect of mass diffusion to the existing equations make this research work as a pioneering work in second grade fluid which no researchers have considered it before to the best of our knowledge.

Mathematical Formulation

A two dimensional laminar flow of an incompressible, electrically conduction MHD viscoelastic liquid due to stretching sheet through porous medium of permeability k_1 is considered with heat transfer when the fluid remains stationary. The sheet is stretched with a velocity $u_w(x)=bx$ where b is a real number. The constant mass transfer velocity is denoted by v_w $with v_w>0$ $for injection and v_w<0$ $for suction$. We choose x-axis along the stretching surface and y-axis perpendicular to the x-axis. The present flow consideration of second grade fluid is governed by the following expressions:

$$\frac{\partial u}{\partial x}+\frac{\partial v}{\partial y}=0 \qquad \text{.......................................(1)}$$

$$u\frac{\partial u}{\partial x}+v\frac{\partial u}{\partial y}=\upsilon\frac{\partial^2 u}{\partial y^2}+\frac{\alpha_1}{\rho}\left(\frac{\partial u}{\partial x}\frac{\partial^2 u}{\partial y^2}+u\frac{\partial^3 u}{\partial x\partial y^2}+\frac{\partial u}{\partial y}\frac{\partial^2 v}{\partial y^2}+v\frac{\partial^3 u}{\partial y^3}\right)-\sigma_1\frac{B_0^2}{\rho}u-\frac{\upsilon}{k_1}u \qquad \text{................(2)}$$

$$u\frac{\partial T}{\partial x}+v\frac{\partial T}{\partial y}=\alpha\frac{\partial^2 T}{\partial y^2}+\mu\left(\frac{\partial u}{\partial y}\right)^2-\frac{\alpha}{\rho}\frac{\partial q_r}{\partial y}+\frac{Q}{\rho c_p}(T-T_\infty)-\sigma\frac{\alpha_1}{\rho}\left\{\frac{\partial u}{\partial y}\frac{\partial}{\partial y}\left(u\frac{\partial u}{\partial x}+v\frac{\partial u}{\partial y}\right)\right\} \qquad \text{.............................(3)}$$

$$u\frac{\partial C}{\partial x}+v\frac{\partial C}{\partial y}=Dm\frac{\partial^2 C}{\partial y^2}+\frac{Dmk_T}{Tm}\frac{\partial^2 T}{\partial y^2}-R^*(C-C_\infty) \qquad \text{...........(4)}$$

Where u and v denote the velocity components in the x- and y-direction, α_1 is the second grade parameter, σ is the coefficient of elastic deformation term, μ is the viscosity coefficient, υ is the kinematic viscosity, σ_1 is the electrical conductivity, ρ is the density of the fluid, α is the thermal diffusivity, c_ρ is the specific heat at constant temperature , T is the fluid temperature, υ is the kinematics viscosity of the fluid, *Q* is the heat release per unit per mass, *g* is the gravitational acceleration, q_r is the radiative heat flux, $R^*$is coefficient of the chemical reaction parameter, and Dm is the coefficient of mass diffusivity, respectively.

The appropriate boundary conditions are considered in the following forms:

$$u=u_w(x)=bx,\quad v=v_w,\quad -k\frac{\partial T}{\partial y}=h(T-T_f),C=Cw \quad at\ y=0$$

$$u=0,\quad \frac{\partial u}{\partial y}=0,\quad T\to T_\infty,\quad C\to C_\infty \qquad at\ y\to\infty$$

.....(5)

Here k is the thermal conductivity of the fluid, h- the convective heat transfer coefficient, V_w- the wall heat transfer velocity, and T_f- the convective fluid temperature below the moving sheet.

The radiative heat flux q_r is described by Roseland approximation such that

$$q_r=-\frac{4\sigma^*}{3K}\frac{\partial T^4}{\partial y}, \qquad \text{................(6)}$$

where σ^* and K are the Stefan-Boltzmann constant and the mean absorption coefficient, respectively. Following Olanrewaju and Abbas (2014), we assume that the temperature differences within the flow are sufficiently small so that the T^4 can be expressed as a linear function after using Taylor series to expand T^4 about the free stream temperature T_∞ and neglecting higher-order terms. This result is the following approximation:

$$T^4 \approx 4T_\infty^3 T - 3T_\infty^4 . \quad \text{.............(7)}$$

Using (5) and (6) in (3), we obtain

$$\frac{\partial q_r}{\partial y} = -\frac{16\sigma^*}{3K}\frac{\partial^2 T^4}{\partial y^2}. \quad \text{................(8)}$$

In order to obtain the similarity solution of the research problem, the following non-dimensional variables are introduced as follows

$$u = axf'(\eta),\ \ v = -\sqrt{a\upsilon}\, f(\eta),\ \ \theta = \frac{T - T_\infty}{T_f - T_\infty},\ C = \frac{C - C_\infty}{C_f - C_\infty},\ \eta = y\sqrt{\frac{a}{\upsilon}} \quad \text{...(9)}$$

where prime symbol denotes differentiation with respect to η and $Re_x = U_\infty x/\upsilon$ is the local Reynolds number. Eqs. (1) – (9) reduce to;

$$f''' + ff'' - f'^2 + K\left(f'f''' - f''^2 - ff^{iv}\right) - \left(M_n + P\right)f' = 0 \quad \text{...(10)}$$

$$(1+R)\theta'' + \Pr f\theta' + \Pr Ecf''^2 + \Pr\lambda\theta - \Pr EcK\delta_1\{f'f''^2 - ff''f'''\} = 0 \quad \text{....................(11)}$$

$$\phi'' + Scf\phi' + ScSr\,\theta'' - \xi Sc\,\phi = 0 \quad \text{.............(12)}$$

Satisfying the conditions

$$f = S,\ \ f' = \frac{b}{a} = \alpha_2,\ \ \theta' = -\gamma[1-\theta(0)],\ \phi = 0,\ at\ \eta = 0$$

$$f' = 0,\ \ f'' = 0,\ \ \theta = 0,\ \ \ \phi = 0\ \ at\ \ \eta \to \infty \quad \text{....(13)}$$

Where

$K = \frac{\alpha_1 a}{\rho\upsilon}$ is the second grade parameter

$M_n = \frac{\sigma B_0^2}{\rho a}$ is the magnetic field parameter

$P = \frac{\upsilon}{k_1 a}$ is the porosity material parameter

$\Pr = \frac{\upsilon}{\alpha}$ is the Prandtl Number

$Ec = \frac{\mu a x^2}{\upsilon(T_f - T_\infty)}$ is the Eckert number

$\delta_1 K = \frac{\sigma\alpha_1 a^2}{\rho\upsilon}$ is the product of the elastic deformation and the second grade parameters

$R = \frac{16\sigma_1 T_\infty^3}{3m\alpha}$ is the thermal radiation parameter

$\lambda = \frac{Q}{\rho c_\rho a}$ is the internal heat generation

$Sc = \frac{\upsilon}{Dm}$ is the Schmitz number

$Sr = \frac{Dmk_T}{\upsilon Tm}\left(\frac{T_f - T_\infty}{C_f - C_\infty}\right)$ is the Soret number

$\xi = \frac{R^*}{a}$ is the chemical reaction parameter

Again, S is the suction and α_2 is the boundary constant

Method of Solution

The coupled non-linear equations (8), (13) and (16) with the boundary conditions in Eq. (17) are solved numerically using the classical Runge-Kutta method with a shooting technique and implemented on Maple (Heck, 2003). The step size 0.001 is used to obtain the numerical solution with seven-decimal place accuracy as the criterion of convergence.

Now, we convert the boundary value problem to an initial value problem by making the following assumption.

Let

$$\begin{pmatrix} X1 \\ X2 \\ X3 \\ X4 \\ X5 \\ X6 \\ X7 \\ X8 \\ X9 \end{pmatrix} = \begin{pmatrix} \eta \\ f \\ f' \\ f'' \\ f''' \\ \theta \\ \theta' \\ \phi \\ \phi' \end{pmatrix} \quad \text{...............................(18)}$$

Satisfying the initial conditions

$$\begin{pmatrix} X1(0) \\ X2(0) \\ X3(0) \\ X4(0) \\ X5(0) \\ X6(0) \\ X7(0) \\ X8(0) \\ X9(0) \end{pmatrix} = \begin{pmatrix} 0 \\ f(0) \\ f'(0) \\ f''(0) \\ f'''(0) \\ \theta(0) \\ \theta'(0) \\ \phi(0) \\ \phi'(0) \end{pmatrix} = \begin{pmatrix} 0 \\ S \\ \alpha_2 \\ \xi \\ \varsigma \\ \tau \\ \tau_1 \\ 0 \\ \tau_2 \end{pmatrix} \quad \text{.........(19)}$$

We differentiate equation (18) with respect to η in order to have the following systems of equations

$$\begin{pmatrix} X1' \\ X2' \\ X3' \\ X4' \\ X5' \\ X6' \\ X7' \\ X8' \\ X9' \end{pmatrix} = \begin{pmatrix} 1 \\ f' \\ f'' \\ f''' \\ f^{iv} \\ \theta' \\ \theta'' \\ \phi' \\ \phi'' \end{pmatrix} = \begin{pmatrix} 1 \\ X3 \\ X4 \\ X5 \\ X5 + X2X4 + X3^2 + K\left(X3X5 - X4^2\right) - (Mn + P)X3/KX2 \\ X7 \\ \Pr EcK\delta_1\left(X3X4^2 - X2X4X5\right) - \Pr \lambda X6 - \Pr EcX4^2 - \Pr X2X7/1+R \\ X9 \\ Sc\gamma X8 - ScSr\left(\left(\Pr EcK\delta_1\left(X3X4^2 - X2X4X5\right) - \Pr \lambda X6 - \Pr EcX4^2 - \Pr X2X7\right)/1+R\right) - ScX2X9 \end{pmatrix} \quad \ldots\ldots\ldots(20)$$

Eq. 20 is solved using Runge-Kutta Gill methods of order four with shooting integration technique satisfying eq. 19. We implemented computer program on Maple that generates the table results and graphs representing the parameter analysis.

Results and Discussion

Numerical calculations have carried out for different values of the thermophysical parameters controlling the fluid dynamics in the flow regime. Eq. (20) satisfying eq. (19) was solved by using the classical Runge-Kutta method of order four alongside with the Shooting technique.

In the Table 1, the Numerical values of the skin-friction, the local Nusselt number and the Sherwood number for the flow parameters when S = 0.5, Pr = 0.72, and $\alpha_2 = 0.5$ were discussed. The effects of the second grade fluid parameter K was discussed while other controlling fluid parameters were kept constant (parameter analysis). It is interesting to note at this junction that as the second grade parameter K increases, the skin-friction, Nusselt number (heat transfer at the surface) and the Sherwood number (mass transfer at the surface) increases. It implies that the second grade parameter enhancing the heat and mass transfer at the surface. It was also noted that as the Newtonian heating parameter γ, internal heat generation λ and the Eckert number Ec increases, the heat and mass transfer at the surface decreases. It was observed that as the convective surface boundary condition parameter called Biot number increases, the wall temperature decreases from 6.0, 2.0 and 1.5. We have also observed that as the porosity P and the magnetic field M_n parameters increases, the skin-friction increases while the heat and mass transfer at the wall decreases. From the table, we also observed that as the radiation parameter R increases, the heat and mass transfer increases. Infact, we can say that radiation parameter enhances the heat and mass transfer at the wall. Elastic deformation parameter δ_1 has influence on the heat and mass transfer at the surface. From the study, it was observed that as this so called parameter increases, the heat and mass transfer also increases steadily. Similarly, as the Schmidt number Sc and Soret number Sr increases, the mass transfer at the wall also increases. In another word, we say the so called parameters enhances the rate of mass transfer at the wall. Finally, the chemical reaction parameter ξ has a greater influence on the rate of mass transfer at the wall. It was a reverse influence as against the Schmidt number and the Soret number. Increasing the chemical reaction parameter, the rate of mass transfer at the wall decreases greatly.

Table 1: Numerical values of the skin-friction, the local Nusselt number and the Sherwood number for the flow parameters when S = 0.5, Pr = 0.72, and $\alpha_2 = 0.5$.

K	γ	Ec	P	M_n	R	λ	δ_1	Sc	Sr	ξ	$f''(0)$	$-\theta'(0)$	$\phi'(0)$	$\theta(0)$
0.1	0.1	0.2	0.2	0.5	0.5	0.5	0.2	0.62	0.2	0.1	−0.64303	1.80985	0.14914	5.99999
0.2											−0.60831	1.87987	0.15577	6.00000
0.3											−0.57971	1.94495	0.16182	5.99999
0.2	0.1	0.2	0.2	0.5	0.5	0.5	0.2	0.62	0.2	0.1	−0.60831	1.87987	0.15577	6.00000
	0.5										−0.60831	0.61778	0.05087	2.00000
	1.0										−0.60831	0.46002	0.03776	1.50000
0.2	0.1	0.0	0.2	0.5	0.5	0.5	0.2	0.62	0.2	0.1	−0.60831	1.89312	0.15734	5.99999
		0.2									−0.60831	1.87987	0.15577	6.00000
		0.5									−0.60831	1.85999	0.15341	5.99999
0.2	0.1	0.2	0.2	0.5	0.5	0.5	0.2	0.62	0.2	0.1	−0.60831	1.87987	0.15577	6.00000
			0.7								−0.69517	1.71997	0.14045	6.00000
			1.0								−0.74093	1.65190	0.13367	5.99999
0.2	0.1	0.2	0.2	0.5	0.5	0.5	0.2	0.62	0.2	0.1	−0.60831	1.87987	0.15577	6.00000
				1.0							−0.69517	1.71997	0.14045	6.00000
				2.0							−0.83518	1.53552	0.12164	6.00000
0.2	0.1	0.2	0.2	0.5	0.5	0.5	0.2	0.62	0.2	0.1	−0.60831	1.87987	0.15577	6.00000
					1.0						−0.60831	3.12916	0.30341	5.99999
					2.0						−0.60831	14.68627	1.67809	6.00000
0.2	0.1	0.2	0.2	0.5	0.5	0.5	0.2	0.62	0.2	0.1	−0.60831	1.87987	0.15577	6.00000
						1.0					−0.60831	14.74897	1.50859	5.99999
						1.5					−0.60831	0.70485	−0.18046	5.99999
0.2	0.1	0.2	0.2	0.5	0.5	0.5	0.2	0.62	0.2	0.1	−0.60831	1.87987	0.15577	6.00000
							0.4				−0.60831	1.88048	0.15584	5.99999
							0.6				−060831	1.88110	0.15591	5.99999
0.2	0.1	0.2	0.2	0.5	0.5	0.5	0.2	0.62	0.2	0.1	−0.60831	1.87987	0.15577	6.00000
								1.00			−0.60831	1.88110	0.23245	5.99999
								1.50			−0.60831	1.88110	0.32114	6.00000

0.2	0.1	0.2	0.2	0.5	0.5	0.5	0.2	0.62	0.2	0.1	−0.60831	1.87987	0.15577	6.00000
									0.3		−0.60831	1.88110	0.23387	6.00000
									0.5		−0.60831	1.88110	0.38979	5.99999
0.2	0.1	0.2	0.2	0.5	0.5	0.5	0.2	0.62	0.2	0.1	−0.60831	1.87987	0.15577	6.00000
										0.4	−0.60831	1.88110	0.05739	5.99999
										1.0	−0.60831	1.88110	0.00068	5.99999

Fig. 1 describes the effects of the second grade parameter K on the velocity distribution across the channel while other controlling fluid [illegible] kept constant. It was noted that as K inc[illegible]y boundary layer thickness thickens [illegible]ary layer. Fig. 2 depicts the graph of t[illegible]ainst η for various values of second [illegible] K with other fluid parameters kept constants. We noticed that as this parameter increases, the thermal boundary layer thickness decreases across the flow channel. Fig. 3 represents the effects of second grade parameter K on the concentration distribution. It was noted that as the second grade parameter increases, the concentration boundary layer decreases close to the wall plate and away from the wall plate. Fig. 4 depicts the influence of the magnetic field parameter M_n on the velocity boundary layer thickness and it was discovered that this parameter step down the rate of flow and directly decreasing the velocity boundary layer thickness. Fig. 5 represents the effects of porosity parameter P on the velocity boundary layer thickness. Similar effect was established with Fig. 4. Increasing the porosity values will decrease the velocity boundary layer thickness across the boundary. Fig. 6 depicts the curve of temperature against spanwise coordinate η for varying values of porosity parameter P and fixed values of other controlling fluid parameters. It is interesting to note from the figure that there were sudden jump from point 4 at the wall before decreasing to satisfy the boundary condition. It is noted that increasing this parameter thickens the thermal boundary layer thickness across the flow channel.

———— K = 0.1
ooooo K = 2.0
+++++ K = 5.0

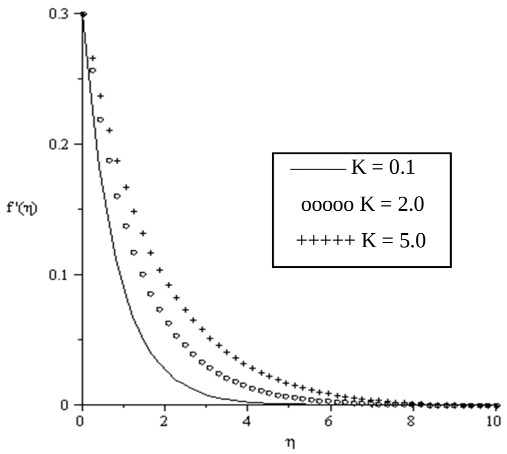

Fig. 1: Velocity distribution for various values of K when $\gamma = 0.1$, Ec = 0.2, P = 0.2, Mn = 0.5, R = 0.5, $\lambda = 0.5$, $\delta_1 = 0.2$, Sc = 0.62, Sr = 0.2, S = 0.5, Pr = 0.72, $\xi = 0.1, \alpha_2 = 0.5$

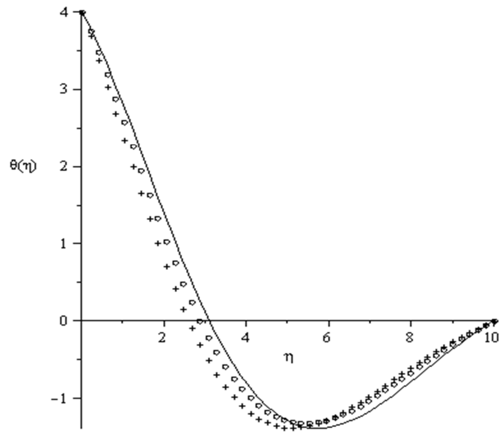

Fig. 2: Temperature distribution for various values of K when $\gamma = 0.1$, Ec = 0.2, P = 0.2, Mn = 0.5, R = 0.5, $\lambda = 0.5$, $\delta_1 = 0.2$, Sc = 0.62, Sr = 0.2, S = 0.5, Pr = 0.72, $\xi = 0.1, \alpha_2 = 0.5$

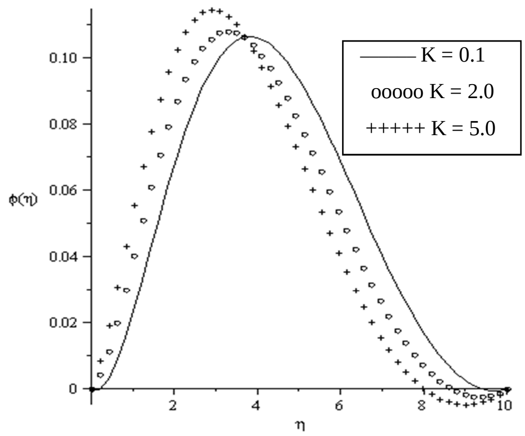

Fig. 3: Concentration distribution for various values of K when $\gamma = 0.1$, Ec = 0.2, P = 0.2, Mn = 0.5, R = 0.5, $\lambda = 0.5$, $\delta_1 = 0.2$, Sc = 0.62, Sr = 0.2, S = 0.5, Pr = 0.72, $\xi = 0.1, \alpha_2 = 0.5$

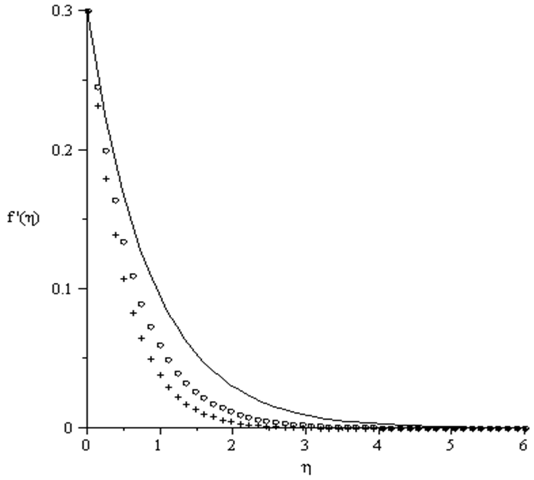

Fig. 4: Velocity distribution for various values of Mn when $\gamma = 0.1$, Ec = 0.2, P = 0.2, K = 0.2, R = 0.5, $\lambda = 0.5,\ \delta_1 = 0.2,$ Sc = 0.62, Sr = 0.2, S = 0.5, Pr = 0.72, $\xi = 0.1, \alpha_2 = 0.5$

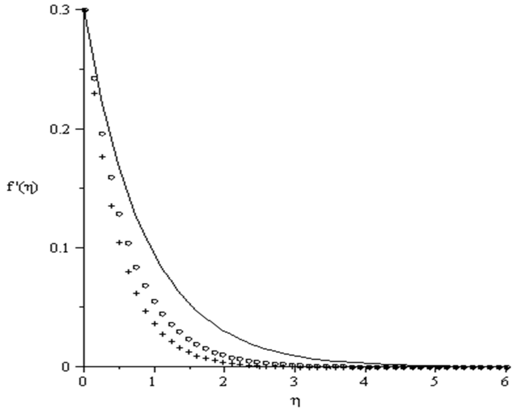

Fig. 5: Velocity distribution for various values of P when $\gamma = 0.1$, Ec = 0.2, Mn = 0.5, K = 0.2, R = 0.5, $\lambda = 0.5,\ \delta_1 = 0.2,$ Sc = 0.62, Sr = 0.2, S = 0.5, Pr = 0.72, $\xi = 0.1, \alpha_2 = 0.5$

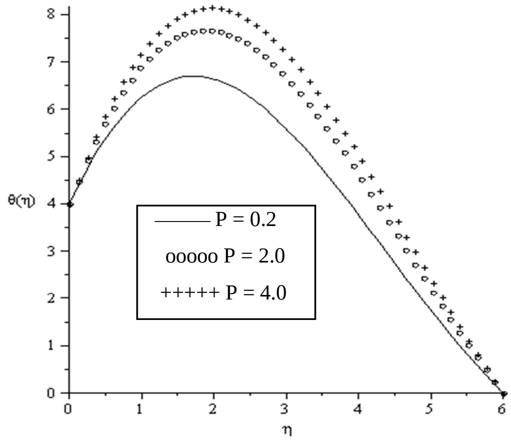

Fig. 6: Temperature distribution for various values of P when $\gamma = 0.1$, Ec = 0.2, Mn = 0.5, K = 0.2, R = 0.5, $\lambda = 0.5,\ \delta_1 = 0.2,$ Sc = 0.62, Sr = 0.2, S = 0.5, Pr = 0.72, $\xi = 0.1, \alpha_2 = 0.5$

Fig. 7 represents graph of temperature distribution with spanwise coordinate η for different values of radiation parameter R. From this Figure, it is seen that the thermal boundary layer thickness decreases across the flowing channel. Fig. 8 depicts ——— Mn = 0.5 ert number Ec on the thermal boundary l ooooo Mn = 2.0 ing the remaining thermophysical param +++++ Mn = 4.0 esting to note a sudden jump close to efore reducing to satisfy the boundary conditions. Increasing the Eckert number thickens the thermal boundary layer thickness across the flow channel. It is also interesting to note that at $\eta > 4$, the reverse was the case towards negative temperature. Figure 9 represents the influence of Eckert number Ec on the concentration distribution. It is interesting to note that as this parameter increases at $0 \le \eta \le 3$, it decreases the concentration boundary layer thickness but at $\eta > 3$, the concentration boundary layer thickness increases. Careful section of this parameter is highly needed by the design engineers. Fig. 10 represents the effects of the internal heat generation λ on the thermal boundary layer boundary. It is interesting to note that when λ = 2, there was a sudden jump close to the wall plate. Similarly, as we increase this internal heat generation parameter, the thermal boundary layer thickness thickened.

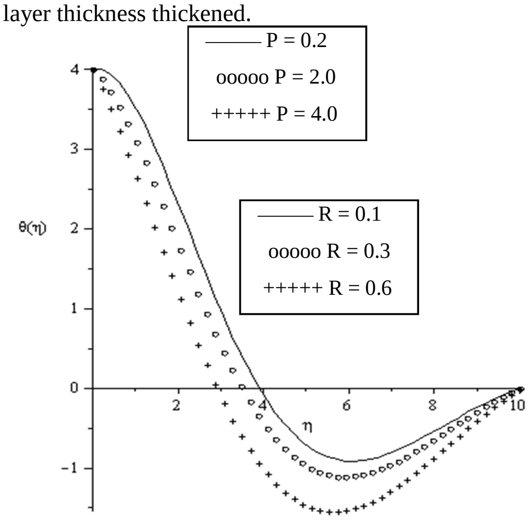

Fig. 7: Temperature distribution for various values of R when $\gamma = 0.1$, Ec = 0.2, Mn = 0.5, K = 0.2, P = 0.2, $\lambda = 0.5,\ \delta_1 = 0.2,$ Sc = 0.62, Sr = 0.2, S = 0.5, Pr = 0.72, $\xi = 0.1, \alpha_2 = 0.5$

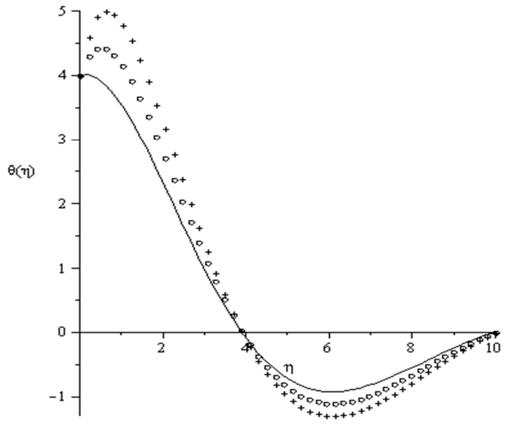

Fig. 8: Temperature distribution for various values of Ec when $\gamma = 0.1$, R = 0.1, Mn = 0.5, K = 0.2, P = 0.2, $\lambda = 0.5$, $\delta_1 = 0.2$, Sc = 0.62, Sr = 0.2, S = 0.5, Pr = 0.72, $\xi = 0.1, \alpha_2 = 0.5$

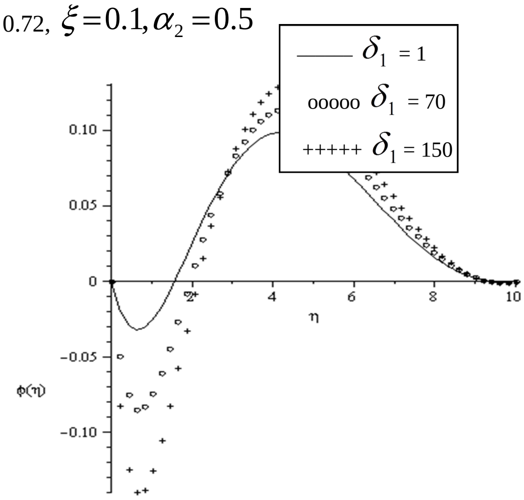

Fig. 9: Concentration distribution for various values of Ec when $\gamma = 0.1$, R = 0.1, Mn = 0.5, K = 0.2, P = 0.2, $\lambda = 0.5$, $\delta_1 = 0.2$, Sc = 0.62, Sr = 0.2, S = 0.5, Pr = 0.72, $\xi = 0.1, \alpha_2 = 0.5$

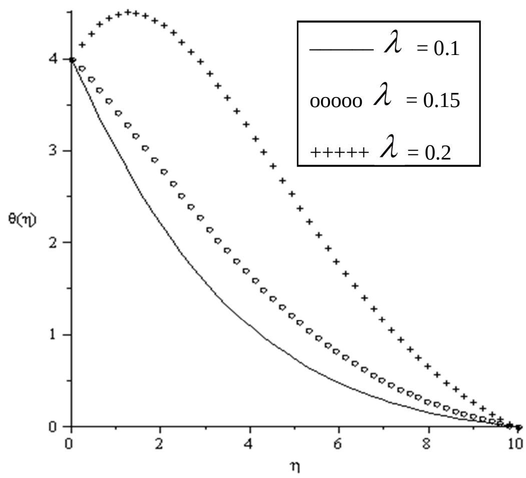

Fig. 10: Temperature distribution for various values of λ when $\gamma = 0.1$, R = 0.1, Mn = 0.5, K = 0.2, P = 0.2, $Ec = 0.4$, $\delta_1 = 0.2$, Sc = 0.62, Sr = 0.2, S = 0.5, Pr = 0.72, $\xi = 0.1, \alpha_2 = 0.5$

Fig. 11 describes the eff[illegible]c deformation parameter δ_1 on the temp[illegible]n while fixing other controlling fluid pa[illegible] channel. It is noted that as the par[illegible] the thermal boundary layer thickness decreases. This parameter was clearly selected in other to notice the difference in the effect on the temperature distribution. Fig. 12 represents the effects of suction parameter S on the velocity distribution. It established the known fact from the literature that suction reduces the rate of flow which resulted in the decreasing the velocity boundary layer flow.

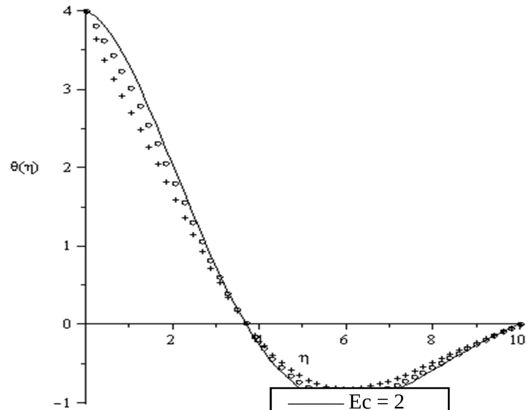

Fig. 11: Temperature distrib[illegible]lues of δ_1 when $\gamma = 0.1$, R = 0.1, [illegible], P = 0.2, $Ec = 0.4$, $\lambda = 0.5$, Sc = 0.62, Sr = 0.2, S = 0.5, Pr = 0.72, $\xi = 0.1, \alpha_2 = 0.5$

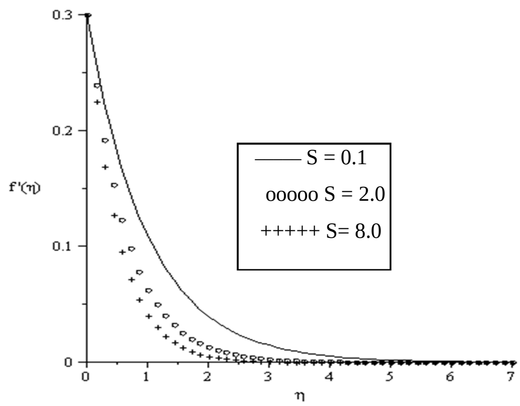

Fig. 12: Velocity distribution for various values of S when $\gamma = 0.1$, R = 0.1, Mn = 0.5, K = 0.2, P = 0.2, $Ec = 0.4$, $\lambda = 0.5$, Sc = 0.62, Sr = 0.2, δ_1 = 0.2, Pr = 0.72, $\xi = 0.1, \alpha_2 = 0.5$

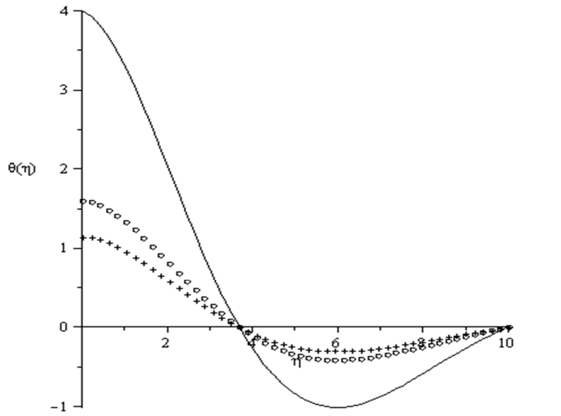

Fig. 13: Temperature distribution for various values of γ when S = 0.5, R = 0.1, Mn = 0.5, K = 0.2, P = 0.2, $Ec = 0.4$, $\lambda = 0.5$, Sc = 0.62, Sr = 0.2, δ_1 = 0.2, Pr = 0.72, $\xi = 0.1, \alpha_2 = 0.5$

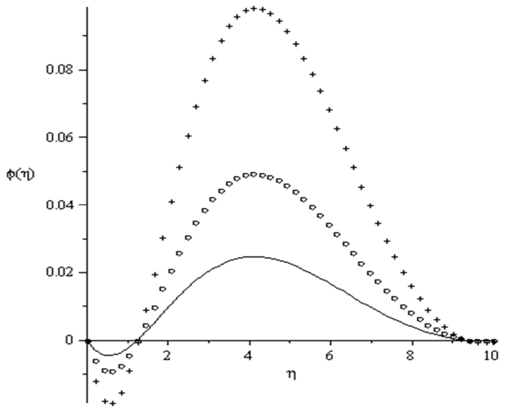

Fig. 14: Concentration distribution for various values of Sr when S = 0.5, R = 0.1, Mn = 0.5, K = 0.2, P = 0.2, $Ec = 0.4$, $\lambda = 0.5$, Sc = 0.62, γ = 0.1, δ_1 = 0.2, Pr = 0.72, $\xi = 0.1, \alpha_2 = 0.5$

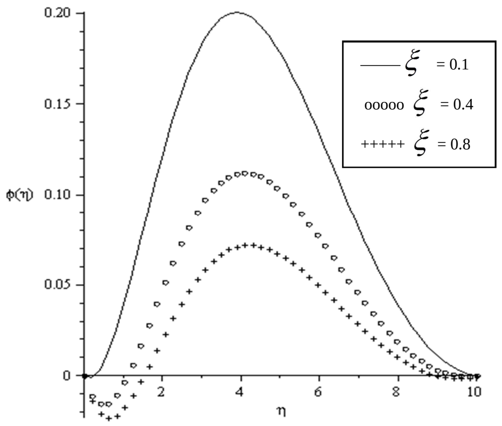

Fig. 15: Concentration distribution for various values of ξ when S = 0.5, R = 0.1, Mn = 0.5, K = 0.2, P = 0.2, $Ec = 0.4$, $\lambda = 0.5$, Sc = 0.62, γ = 0.1, δ_1 = 0.2, Pr = 0.72, $Sr = 0.2, \alpha_2 = 0.5$

Fig. 13 represents the curve of temperature against spanwise coordinate η for varying values of convective surface boundary condition parameter (Biot number) γ and fixed values of oth d parameters. It is noted that as the es, the thermal boundary layer thickne 14 represents the effect of Soret numbe ntration boundary layer thickness. It is interesting to note that as the Soret number increases, the concentration boundary layer thickness decreases along negative direction and increases along positive values of the concentration profile. Fig. 15 depicts the plot of concentration distribution with spanwise coordinate η for different values of chemical reaction parameter ξ for fixed controlling fluid parameters. It is noted that as the chemical reaction parameter increases, the concentration boundary layer thickness decreases across the flow channel.

Conclusions

The double-diffusive convection MHD flow of a second grade fluid with a convective surface boundary condition in the presence of elastic deformation i ium with Soret and chemical reaction ove heet were studied numerically. The radi k is modelled through the non-linear R sion approximation, which produces one ne atio parameter. The present study reveals that this parameter influences velocity temperature and concentration fields significantly. The effects of various physical parameters on fluid flow, heat and mass transfer phenomena have been studied. Finally we arrived at the following major findings:

- The velocity distribution boundary layer thickness thickens across the boundary as the second grade parameter K increases while the temperature and concentration boundary layer thickness decreases. Similarly, the skin-friction coefficient, the heat transfer and the mass transfer rate increases as K increases.
- The velocity profile decreases as the magnetic field Mn and porosity parameters increases while the thermal boundary layer thickness increases. Similarly, the heat and mass transfer rate decreases as both parameters increases across the channel.
- The thermal boundary layer thickness thickens as the internal heat generation λ and the elastic deformation δ_1 parameters increases while the heat and mass transfer rate increases as the elastic deformation parameter increases.
- The Biot number γ representing cooling effect. The rate of heat transfer at the surface increases as this parameter increases while the thermal boundary layer thickness decreases.
- The concentration distribution boundary layer thickness decreases as the Soret number Sr and the chemical reaction parameter ξ increases.
- It is interesting to note that carefully selection of the controlling fluid parameters are needed to get a desirable fluid flow model. The elastic deformation parameter were carefully selected before the effect can be seen or felt on the thermal boundary layer

thickness which invariably increases the heat transfer rate at the surface.

- This model will serve as a benchmark on double-diffusive convection MHD flow on a second grade fluid.

References

Asghar S, Hayat T & Ariel PD 2009. Unsteady couette flows in a second grade fluid with variable material properties. *Comm. Nonlinear Sci. & Numer. Simulation,* 14(1): 154-159.

Aziz A 2009. A similarity solution for laminar thermal boundary layer over a flat plate with a convective surface boundary condition. *Commun. Nonlinear Sci. Numer Simulat.,* 14: 1064–1068.

Aziz A. (2010) Hydrodynamic and thermal slip flow boundary layers over a flat plate with constant heat flux boundary condition. *Commun Nonlinear Sci Numer Simulat*.15:573–580.
doi:10.1016/j.cnsns.2009.04.026

Bataller BC 2008. Radiation effects for Blasius and Sakiadis flows with a convective surface boundary condition. *Appl. Maths. Comput*., 206 832–840.

Bejan A 2004. *Convective Heat Transfer*. 3rd edition John Wiley & Son, New York

David FR 1992. *Laminar Flow Analysis.* Cambridge University Press, New York.

Hayat T, Abbas Z, Sajid M & Asghar S 2007. The influence of thermal radiation on MHD flow of a second grade fluid. *Int. J. Heat Mass Transfer,* 50: 931– 941.

Hayat T, Mambili M & Mahomed FM 2009. A note on some solutions for the flow of a fourth grade fluid in a porous space. *Nonlinear Analysis: Real World Applic.* 10: 368-374.

Hayat T, Qasim M & Abbas Z 2010. Radiation and mass transfer effects on magnetohydrodynamic unsteady flow induced by a shrinking sheet. *Z Naturforsch,* 65a: 231–239.

Hayat T & Qasim M 2010. Influence of thermal radiation and Joule heating on MHD flow of a Maxwell fluid in the presence of thermophoresis. *Int. J. Heat Mass. Transfer,* 53: 4780-4788.

Hayat T, Shehzad SA, Qasim M & Obaidat S 2011. Flow of a second grade fluid with convective boundary conditions. *Thermal Science,* 15(2): S253-S261.

Hayat T & Abbas Z 2008. Heat transfer analysis on the MHD flow of a second grade fluid in a channel with porous medium. *Chaos, Solitons & Fractals,* 38: 556–567.

Hayat T, Abbas Z, Sajid M & Asghar S 2007. The influence of thermal radiation on MHD flow of a second grade fluid. *Int. J. Heat & Mass Transfer,* 50: 931–941.

Hayat T, Ahmed N, Sajid M & Asghar S 2007. On the MHD flow of a second grade fluid in a porous channel. *Computers & Maths. with Applic.,* 54: 407–414.

Hayat T, Shehzad SA, Qasim M & Obaidat S 2011. Flow of a second grade fluid with convective boundary conditions. *Thermal Science,* 15: 253-261.

Heck A 2003. *Introduction to Maple.* 3rd Edition, Springer-Verlag,

Ibrahim SM & Redd NB 2012. Radiation and mass transfer effects on MHD free convection flow along a stretching surface with viscous dissipation and heat generation, *Int. J. Appl. Maths & Mech*., 8(8): 1-21.

Ishak A 2010. Similarity solutions for flow and heat transfer over a permeable surface with convective boundary condition. *Appl. Maths. Comput.* 217: 837–842.

Ishak A, Yacob NA & Bachok N 2010. Radiation effects on the thermal boundary layer flow over a moving plate with convective boundary condition. *Meccanica,* doi:10.1007/s11012-010-9338-4.

Incropera FP, Dewitt DP, Bergman TL & Lavine AS 2007. *Fundamentals of Heat and Mass Transfer*. 6th edition John Wiley, New York.

Magyari E 2011. Comment on “A similarity solution for laminar thermal boundary layer over a flat plate with convective surface boundary condition” by A. Aziz. Comm. *Nonlinear Sci. Numer. Simul.,* 2009; 14; 1064–8, *Comm. Nonlinear Sci. Num. Simul.* 16: 599–601.

Olajuwon BI 2011. Convection heat and mass transfer in a hydromagnetic Flow of a second grade fluid in the presence of thermal radiation and thermal diffusion. *Int. J. Heat Mass Transf.,* 38(3): 377–382.

Olanrewaju PO & Abbas Z 2014. Corrigendum to convection heat and mass transfer in a hydromagnetic flow of a second grade fluid in the presence of thermal radiation and thermal diffusion. *Int. J. Heat Mass Transf.,* 38(3) (2011) 377–382.

Olanrewaju PO, Gbadeyan JA, Hayat T & Hendi AA 2011. Effects of internal heat generation, thermal radiation and buoyancy force on a boundary layer over a vertical plate with a convective surface boundary condition. *S. Afr J. Sci.,* 107(9/10), Art. #476

Raptis A, Perdikis C & Takhar HS 2004. Effects of thermal radiation on MHD flow. *Appl Math. Comput.,* 153: 645–649.

Reddaiah P & Rao DRVP 2012. Convective heat and mass transfer flow of a viscous fluid through a porous medium in an duct-by finite element method. *Int. J Appl. Maths & Mech*., 8(10): 1-27.

Reddaiah P & Rao DRVP 2012. Effect of radiation on Hydromagnetic convective heat transfer flow of a viscous electrically conducting fluid in a non-uniformly heated vertical channel. *Int. J Appl. Maths & Mech*., 8(9): 99-121.

Sharma R, Bhargava R & Singh IV 2012. A numerical solution of MHD convection heat transfer over an unsteady stretching surface in a porous medium using element free gaalerkin method. *Int. J Appl. Maths & Mech*., 8(10): 83-103.

Singh V & Agarwal S 2012. Heat transfer in a second grade fluid over an exponentially stretching sheet through porous medium with thermal radiation and elastic deformation under the effect of magnetic field. *Int. J. of Applied Math and Mech.,* 8(4): 41-63.

Singh G, Sharma P. R 2009. Effects of ohmic heating and viscous dissipation on steady MHD Flow near a stagnation point on an isothermal stretching sheet. *Thermal Science,* 13(1): 5-12.

Subhashini SV & Samuel N Pop I 2011. Double-diffusive convection from a permeable vertical surface under convective boundary condition. *Int. Commun. in Heat & Mass Transfer* 38: 1183–1188.

Shu JJ & Pop I 1988. On thermal boundary layers on a flat plate subjected to a variable heat flux. *Int. J. Heat Fluid Flow* 19: 79–84.

Yao S, Fang T & Zhong Y 2011. Heat transfer of a generalized stretching/shrinking wall problem with convective boundary conditions. *Commun. Nonlinear Sci. Numer. Simulat.* 16(2): 752–760.